Short-range order in amorphous Ni-Zr alloys

F. Paul
Institut für Experimentalphysik der Christian-Albrechts-Universität Kiel, Leibnizstrasse 19, D-2300 Kiel 1, West Germany

R. Frahm
Hamburger Synchrotronstrahlungslabor (HASYLAB) at Deutsches Elektronen-Synchrotron (DESY), Notkestrasse 85, D-2000 Hamburg 52, West Germany

(Received 7 February 1990)

The short-range order in amorphous $Ni_{24.1}Zr_{75.9}$, $Ni_{33.3}Zr_{66.7}$ and $Ni_{36.5}Zr_{63.5}$ alloys was investigated by anomalous x-ray scattering. The partial coordination numbers and interatomic distances are compared with the results of extended x-ray-absorption fine-structure measurements. The pair-correlation function of a heat-treated $Ni_{36.5}Zr_{63.5}$ alloy shows a more pronounced structure and a larger correlation length than the as-cast alloy but is still typical for amorphous solids.

INTRODUCTION

Ni-Zr glasses are typical examples of amorphous metal-metal alloys. The local atomic environment in a material consisting of n components is well described by the $n(n+1)/2$ partial distribution functions, from which interatomic distances and partial coordination numbers can be calculated. A binary compound is described by three independent pair-correlation functions. In neutron-scattering experiments the strongly varying neutron-scattering length of Ni in Ni-Zr alloys was used to resolve partial structure factors.[1-3] In differential anomalous x-ray-scattering measurements[4,5] (DAS) changes in the scattering factors at different photon energies at the Ni and the Zr K edges lead to partial atomic distribution functions. Also measurements of the extended x-ray-absorption fine structure (EXAFS) of $Ni_xZr_{(100-x)}$ samples with nominal composition $x=24.1$, 33.3, and 36.5 (Ref. 6) revealed the element specific coordination. Additionally the structural changes during the crystallization of a $Ni_{36.5}Zr_{63.5}$ alloy were investigated by Frahm, Haensel, and Rabe.[7] They heated the metallic glass in an apparatus for differential scanning calorimetry (DSC) and demonstrated the existence of an intermediate amorphous state after the first of two exothermic reactions.[8] To evaluate partial coordination numbers and interatomic distances in those Ni-Zr alloys we performed x-ray-diffraction measurements applying the anomalous scattering technique at a conventional x-ray generator. The characteristic Au $L\alpha_1$ and Mo $K\alpha_1$ lines were used to change the scattering factors of Ni and Zr.

THEORETICAL BACKGROUND

The total structure factor $S(q)$ of an amorphous solid can be determined from the coherently scattered intensity $I_{\rm coh}(q)$ using the definition of Faber and Ziman[9]

$$S(q)-1=\frac{I_{\rm coh}(q)-\langle f^2(q)\rangle}{\langle f(q)\rangle^2} \ . \tag{1}$$

Here $q=(4\pi/\lambda)\sin\theta$ denotes the modulus of the scattering vector as a function of the scattering angle 2θ and x-ray wavelength λ. The mean and mean-squared scattering factors $\langle f(q)\rangle$ and $\langle f(q)^2\rangle$ are determined for a binary system by the concentrations c_i and the scattering factors f_i of the constituents Ni ($i=1$) or Zr ($i=2$) by $f=c_1f_1+c_2f_2$ and $f^2=c_1f_1^2+c_2f_2^2$, respectively.

The total structure factor $S(Q)$ is the weighted sum of three partial structure factors

$$S(q)-1=\sum_i\sum_j\frac{c_ic_jf_if_j}{\langle f\rangle^2}S_{ij}(q)-1 \ , \tag{2}$$

where the partial structure factors $S_{ij}(q)$ refer to atom pairs of type ij. The Fourier transform of the q-weighted total structure factor results in the reduced radial distribution function

$$G(r)=4\pi r[\rho(r)-\rho_0]$$
$$=\frac{2}{\pi}\int_0^\infty q[S(q)-1]\sin(qr)dq \ , \tag{3}$$

where $\rho(r)$ is the radial number density function in atoms/Å^3 and ρ_0 the average number density. Similar to the total structure factor $\rho(r)$ is the weighted sum of three partial radial density functions

$$\rho(r)=\sum_i\sum_j\frac{c_if_if_j}{\langle f\rangle^2}\rho_{ij}(r) \ . \tag{4}$$

The weighting factors are different from those of Eq. (2) which has an additional factor c_j.

For a discussion of the atomic structure of amorphous solids it is useful to introduce the radial distribution function

$$Z(r)=4\pi r^2\rho(r) \ . \tag{5}$$

From the area of the first peak in the $Z(r)$ the total coordination number N of the next-nearest neighbors can be

 ©1990 The American Physical Society

TABLE I. The $f'(E)$ and $f''(E)$ values in electron units for the used photon energies calculated from the absorption data given by McMaster *et al.* (Ref. 11).

	Ni		Zr	
	f'	f''	f'	f''
Au $L\alpha_1$ (9.712 keV)	−0.94	3.06	−0.56	1.67
Mo $K\alpha_1$ (17.479 keV)	0.30	1.13	−3.08	0.56

calculated according to

$$N=\int_{r_1}^{r_2} Z(r)dr \ , \tag{6}$$

where the minima preceding and following the first peak were taken as integration limits r_1 and r_2. This procedure is not rigorously defined, hence a moderate uncertainty in determination of N results.[10] The total coordination number N is a linear sum of the three partial coordination numbers

$$N=\sum_i \sum_j \frac{c_i f_i f_j}{\langle f \rangle^2} N_{ij} \ . \tag{7}$$

The values N_{ij} represent the partial coordination numbers of the atoms of type j around atoms of type i with the relation $c_i N_{ij}=c_j N_{ji}$. The weighting factors $c_i f_i f_j/\langle f \rangle^2$ in Eq. (7) as well as Eq. (2) can be varied by the anomalous dispersion of x-rays. In the nonrelativistic theory the scattering factor f can be written as $f(q,E)=f_0(q)+f'(E)+if''(E)$, where $f'(E)$ is the anomalous correction to the scattering, $f''(E)$ corresponds to the absorption, and E is the photon energy. The term $f'(E)$ is related to $f''(E)$ by the Kramers-Kronig transformation and varies strongly in the neighborhood of absorption edges. The EXAFS at the Ni and Zr K edges usually modulates f', but has no influence on f'' in our case because the photon energies used in our experiments (Au $L\alpha_1$ and Mo $K\alpha_1$ lines) are far away from both edges. Nevertheless a sufficient variation of the weighting factors in Eq. (7) was obtained to allow the calculations of partial distances and coordination numbers.

The absorption of the sample was calculated using the compilation of x-ray cross sections by McMaster *et al.*[11] From those data the values for $f''(E)$ and $f'(E)$ listed in Table I were determined applying the method described by Dreier *et al.*[12] The advantage of determining partial coordination numbers from Eq. (7) instead of performing a matrix inversion of Eq. (2) is the fact that Eq. (7) is nearly independent of q and causes no numerical problems.

EXPERIMENT AND DATA EVALUATION

The scattering experiments were done with x rays from a Rigaku RU 200 PL rotating anode x-ray generator equipped with Au or Mo targets. Samples with a typical width of 5 mm and a thickness of 40 μm were mounted on a frame which was large enough to avoid scattering from the sample holder. The diffraction data were measured at room temperature (20 °C) in reflection geometry using a Si(Li) solid-state detector. To reduce the contribution of fluorescent radiation in the diffraction pattern the pulse height was discriminated by a multichannel analyzer. The scattering angle covered the range from 2° to 65° corresponding to a maximum wave number $q_{max}=8.9$ Å^{-1} for Au $L\alpha_1$ and $q_{max}=16.1$ Å^{-1} for Mo $K\alpha_1$ radiation. The measured intensities were corrected for air scattering, polarization, and absorption. Multiple scattering was approximated by the procedure described by Dwiggins and Park.[13] Considering also inelastic scattering the data were normalized by the Krogh-Moe-Norman method.[14,15] A damping factor $\exp(-\alpha q^2)$ with $\alpha=0.005$ Å^2 was used in the Fourier transform to reduce termination ripples in the transformed data. The average number densities ρ_0 required in Eq. (3) were calculated from the macroscopic densities published by Altounian and Strom-Olsen.[16]

RESULTS AND CONCLUSIONS

The corrected and normalized diffraction patterns for the Ni-Zr samples which are typical for amorphous materials are shown in Fig. 1. In the structure factors (Fig. 2) very small peaks probably due to crystalline material at the surface of some ribbons can be seen but do not affect the correlation functions in r space. The structure factors of the as-cast samples are very similar. Comparing the DSC-treated sample with the others, the DSC-

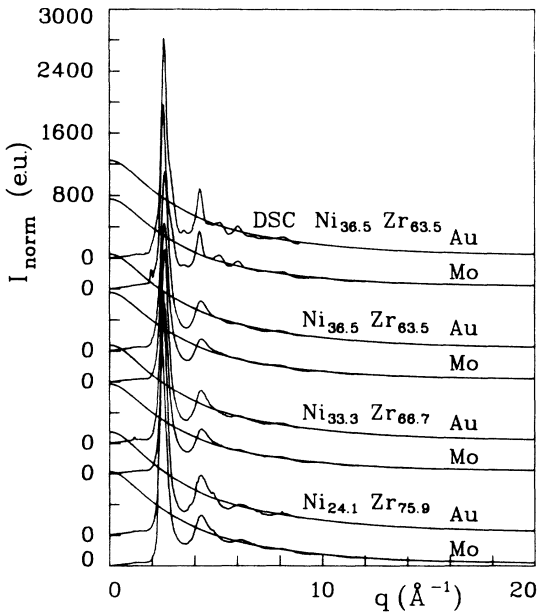

FIG. 1. Corrected and normalized intensities of the amorphous $Ni_xZr_{(100-x)}$ alloys and a DSC-treated sample for the Au $L\alpha_1$ (9.712 keV) and the Mo $K\alpha_1$ lines (17.479 keV).

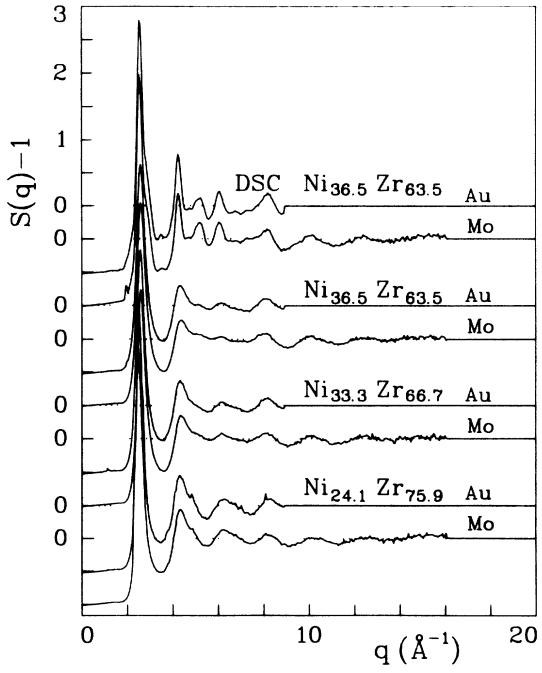

FIG. 2. Structure factors of the amorphous $Ni_xZr_{(100-x)}$ alloys and a DSC-treated sample for the Au $L\alpha_1$ (9.712 keV) and the Mo $K\alpha_1$ lines (17.479 keV); calculation according to Faber and Ziman (Ref. 9).

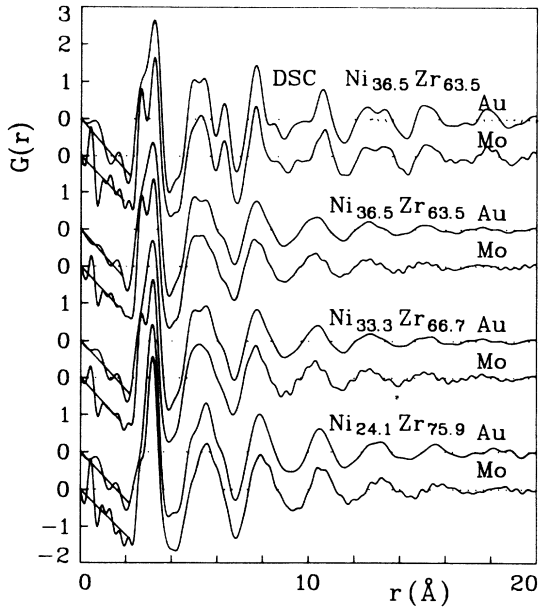

FIG. 3. Reduced radial pair distribution functions $G(r)$ of the amorphous $Ni_xZr_{(100-x)}$ alloys and a DSC-treated sample for the Au $L\alpha_1$ (9.712 keV) and the Mo $K\alpha_1$ lines (17.479 keV).

treated alloy has a more pronounced structure up to about 8 Å^{-1}. From the full width at half maximum of the first peak Δq_1, a range of topological short-range order χ_1 can be calculated by $\chi_1 = \Delta q_1 / 2\pi$. For the DSC-treated sample a value of 18 Å results, whereas for the as-cast samples 14 Å is determined. Parameters which were derived from the structure factors are given in Table II. The reduced radial distribution functions $G(r)$ are obtained by Fourier transforms of $S(q)-1$ and are displayed in Fig. 3. Although the spatial resolution of the measurements with the Au-emission line is not as good as that with the Mo-emission line, the change upon the concentration of Ni can be recognized very well. The first peak at $r = 2.70$ Å is due to the Ni-Zr correlation. Its height decreases with a decreasing amount of Ni and is reduced to a small shoulder in the case of $Ni_{24.1}Zr_{75.9}$. Accordingly, the height of the second maximum at $r = 3.00$ Å, which characterizes the Zr-Zr correlation, increases. The reduced radial distribution function $G(r)$ of the DSC-treated Ni-Zr alloy differs significantly from the as-cast samples: The nearest-neighbor peaks for DSC-treated Ni-Zr are higher and sharper than the ones for the untreated alloys. Furthermore, in the range from 4 to 12 Å additional relatively sharper features show up. This indicates that the local coordination is more defined in the annealed sample than in the as-cast alloys.

From $G(r)$ the interatomic distances were derived with an accuracy of ±0.02 Å, whereas from the areas of the first maxima in the radial distribution function $Z(r)$ (see

TABLE II. Positions q_1 and q_2 of the first and second maximum in the structure factor of the amorphous as-cast $Ni_xZr_{(100-x)}$ alloys and the DSC-treated sample. The correlation length χ_1 was calculated from the width Δq_1 of the first maximum. The interatomic distances r and coordination numbers N were calculated as discussed in the text.

Alloy	E (keV)	q_1 (Å^{-1})	q_2 (Å^{-1})	Δq_1 (Å^{-1})	χ_1 (Å)	r_1 (Å)	N_1	r_2 (Å)	N_2
$Ni_{24.1}Zr_{75.9}$	9.712	2.55	4.35	0.43	14.6	−/3.16	12.95	5.35	50.2
	17.479	2.50	4.35	0.43	14.6	2.70/3.16	13.20	5.58	49.4
$Ni_{33.3}Zr_{66.7}$	9.712	2.60	4.35	0.50	12.6	−/3.16	13.40	5.00	51.1
	17.479	2.60	4.35	0.45	14.0	2.70/3.16	12.80	5.31	49.7
$Ni_{36.5}Zr_{63.5}$	9.712	2.60	4.35	0.80	7.9	−/3.16	13.40	5.00	50.2
	17.479	2.61	4.40	0.45	14.0	2.67/3.19	13.00	5.03	50.8
DSC $Ni_{36.5}Zr_{63.5}$	9.712	2.55	4.25	0.35	18.0	−/3.22	13.75	4.97	56.1
	17.479	2.55	4.20	0.35	18.0	2.70/3.25	13.40	5.28	56.2

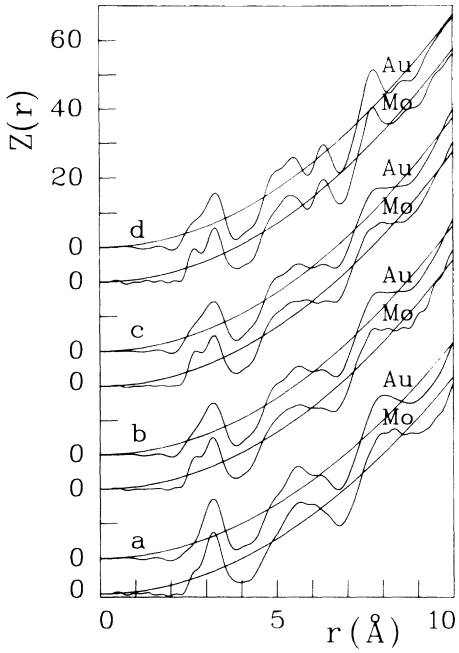

FIG. 4. Radial distribution functions $Z(r)$. (a) $Ni_{24.1}Zr_{75.9}$, (b) $Ni_{33.3}Zr_{66.7}$, (c) $Ni_{36.5}Zr_{63.5}$, and (d) DSC-treated $Ni_{36.5}Zr_{63.5}$ for the Au $L\alpha_1$ (9.712 keV) and the Mo $K\alpha_1$ lines (17.479 keV).

Fig. 4) the total coordination numbers were calculated with an accuracy of ± 0.1. The results are given in Table II. Those areas can be used to calculate partial coordination numbers of all four samples by Eq. (7). Since in earlier investigations[1,2,4,6] it was found that either the Ni-Ni coordination cannot be determined or that it is very small, we neglected this component. Therefore only two linear equations that contain the Zr-Ni and the Zr-Zr coordinations are necessary to determine the remaining independent coordination numbers $N_{\text{Ni-Zr}}$ and $N_{\text{Zr-Zr}}$ and thus measurements at two different photon energies are sufficient. Using the values of f' given in Table I and the atomic concentrations of the elements the following system of linear equations was derived: for $Ni_{24.1}Zr_{75.9}$

$$\begin{aligned} N_{\text{Au}} &= 1.139 N_{\text{Zr-Ni}} + 0.920 N_{\text{Zr-Zr}} , \\ N_{\text{Mo}} &= 1.362 N_{\text{Zr-Ni}} + 0.827 N_{\text{Zr-Zr}} , \end{aligned} \tag{8a}$$

for $Ni_{33.3}Zr_{66.7}$

$$\begin{aligned} N_{\text{Au}} &= 1.081 N_{\text{Zr-Ni}} + 0.875 N_{\text{Zr-Zr}} , \\ N_{\text{Mo}} &= 1.236 N_{\text{Zr-Ni}} + 0.753 N_{\text{Zr-Zr}} , \end{aligned} \tag{8b}$$

and for $Ni_{36.5}Zr_{63.5}$

$$\begin{aligned} N_{\text{Au}} &= 1.059 N_{\text{Zr-Ni}} + 0.875 N_{\text{Zr-Zr}} , \\ N_{\text{Mo}} &= 1.191 N_{\text{Zr-Ni}} + 0.840 N_{\text{Zr-Zr}} . \end{aligned} \tag{8c}$$

The partial coordination numbers calculated by these equations are given in Table III. Considering an error in the total coordination number of ± 0.1 one obtains in the case of $Ni_{33.3}Zr_{66.7}$ for $N_{\text{Zr-Ni}}$ a value of 4.2 ± 0.6 and for $N_{\text{Zr-Zr}}$ in the same manner 10.1 ± 0.9. The error in the partial coordination numbers in case of the other alloys is of the same order.

These results can be compared with EXAFS measurements of Frahm, Haensel, and Rabe[6,7] and scattering investigations of amorphous Ni-Zr alloys by other authors which are summarized in Table III. It can be seen that the coordination numbers in the present study agree with the results of scattering experiments of Lee, Jost, and Wagner[2] and de Lima *et al.*[4] Only the interatomic dis-

TABLE III. Interatomic distances and partial coordination numbers of the as-cast $Ni_xZr_{(100-x)}$ alloys and the DSC-treated sample in comparison to published results.

		Ni-Ni		Ni-Zr		Zr-Ni		Zr-Zr	
	Alloy	r (Å)	N	r (Å)	N	r (Å)	N	r (Å)	N
This work	$Ni_{24.1}Zr_{75.9}$			2.70	14.5	2.70	4.6	3.16	8.4
	$Ni_{33.3}Zr_{66.7}$			2.70	8.3	2.70	4.2	3.16	10.1
	$Ni_{36.5}Zr_{63.5}$			2.70	9.6	2.70	5.6	3.16	8.6
	DSC $Ni_{36.5}Zr_{63.5}$			2.70	10.5	2.70	6.0	3.24	8.6
Frahm, Haensel, and Rabe (Ref. 6)	$Ni_{24.1}Zr_{75.9}$			2.62	2.35	2.62	0.84	3.17	9.66
	$Ni_{33.3}Zr_{66.7}$			2.62	2.39	2.62	1.43	3.18	10.10
	$Ni_{36.5}Zr_{63.5}$			2.62	2.44	2.62	1.56	3.20	8.91
Frahm, Haensel, and Rabe (Ref. 7)	DSC $Ni_{36.5}Zr_{63.5}$			2.63	3.15	2.63	1.81	3.21	5.97
Lee *et al.* (Ref. 1)	$Ni_{35}Zr_{65}$	2.66	2.3	2.69	5.4	2.69	2.9	3.15	9.0
Lee *et al.* (Ref. 2)	$Ni_{35}Zr_{65}$	2.66	2.3	2.69	7.9	2.69	4.3	3.15	9.1
de Lima *et al.* (Ref. 4)	$Ni_{25}Zr_{75}$		<1.3	2.76	12.6	2.76	4.2	3.23	11.0

tances for the Ni-Zr and Zr-Ni distances in the $Ni_{25}Zr_{75}$ alloy (de Lima *et al.*[4]) differ from our measurements. The coordination numbers for the Zr-Zr correlation which follows from the EXAFS analysis[6,7] are in agreement with our diffraction experiments. However, the structural parameters for the unlike atoms are significantly different from our diffraction experiments. As extensively discussed in the literature about EXAFS investigations of metallic glasses[6,17–20] this can be due to non-Gaussian pair distribution functions, which are difficult to investigate with EXAFS. The EXAFS method probes the high values in momentum space, making it more sensitive to the broadening of pair-correlation functions and thus long-range order information may be lost. Information about broader radial peaks can be extracted from x-ray-scattering data where the wave-number space extends nearly to zero.[18–20] Those differences make a direct comparison of the structural data obtained by both methods difficult in the case of amorphous materials. The repulsive part of the pair potential gives rise to narrower distance distributions. As in the current case thus the interatomic distances in the case of metallic glasses obtained by evaluation of EXAFS spectra are generally smaller than the results of x-ray diffraction. In the Gaussian approximation, which is used in the standard EXAFS analysis, only a fraction of the pair distribution can be observed, which is also indicated by an apparent low Ni-Zr coordination number. The small width of the pair distribution was interpreted by Frahm, Haensel and Rabe[6] as an indication for a strong Ni-Zr interaction.

Comparing our results for the as-cast and the annealed $Ni_{36.5}Zr_{63.5}$ alloys it can be seen that the Ni-Zr distance remains constant, whereas the Zr-Ni coordination number increases by about 7%. The Zr-Zr distances, however, increase by 0.08 Å, whereas the coordination number remains constant. The EXAFS results for the same samples of Frahm, Haensel, and Rabe[7] also show a constant Ni-Zr bond length upon passing the first DSC peak and an increasing Ni-Zr coordination number. The decrease in the apparent Zr-Zr coordination number in the EXAFS results is due to major atomic rearrangements in this shell, which may be interpreted as the creation of a non-Gaussian pair distribution function. Thus qualitatively both methods indicate similar structural changes upon annealing, whereas the absolute structural parameters derived from our x-ray-diffraction work are supposed more reliable as discussed above. The EXAFS data were interpreted in terms of the existence of structural units and chemical bonding between unlike atoms in the amorphous Ni-Zr alloys. The present investigation supports this conclusion by the stability of the Ni-Zr bond length upon annealing, whereas the Zr-Zr bond length changes significantly.

[1]A. E. Lee, G. Etherington, and C. N. J. Wagner, J. Non-Cryst. Solids **61&62**, 349 (1984).
[2]A. E. Lee, S. Jost, and C. N. J. Wagner, J. Phys. (Paris) Colloq. **46**, C8-181 (1985).
[3]R. Bellisent, J. Bigot, Y. Calvayrac, S. Lefebvre, and A. Quivy, J. Phys. (Paris) Colloq. **46**, C8-87 (1985).
[4]J. C. de Lima, D. Raoux, Y. Charreire, and M. Maurer, Z. Phys. Chemie **157**, 65 (1988).
[5]J. C. de Lima, J. M. Tonnerre, and D. Raoux, J. Non-Cryst. Solids **108**, 38 (1988).
[6]R. Frahm, R. Haensel, and P. Rabe, J. Phys. F **14**, 1333 (1984).
[7]R. Frahm, R. Haensel, and P. Rabe, J. Phys. Condens. Matter **1**, 1521 (1989).
[8]R. Frahm, J. Non-Cryst. Solids **56**, 255 (1983).
[9]T. E. Faber and J. M. Ziman, Philos. Mag. **11**, 153 (1965).
[10]Y. Waseda, *The Structure of Non-Crystalline Materials, Liquids and Amorphous Solids* (McGraw-Hill, New York, 1980).
[11]W. H. McMaster, N. Kerr del Grande, J. H. Mallet, and J. H. Hubbel, Lawrence Livermore Laboratory Report No. UCRL-50174-SEC2-R1, 1969 (unpublished).
[12]P. Dreier, P. Rabe, W. Malzfeldt, and W. Niemann, J. Phys. C **18**, 3123 (1984).
[13]C. W. Dwiggins and D. A. Park, Acta Cryst. A **27**, 264 (1971).
[14]J. Krogh-Moe, Acta Cryst. **9**, 951 (1956).
[15]N. Norman, Acta Cryst. **10**, 370 (1957).
[16]Z. Altounian and J. O. Strom-Olsen, Phys. Rev. B **27**, 4149 (1983).
[17]R. Haensel, P. Rabe, G. Tolkiehn, and A. Werner, in *Liquid and Amorphous Metals,* edited by E. Lüscher and H. Coufal (Sijthoff & Nordhoff, Alphen aan den Rijn, 1980), p. 459.
[18]G. S. Cargill, W. Weber, and R. F. Boehme, in *EXAFS and Near Edge Structure,* edited by A. Bianconi, L. Incoccia, and S. Stipcich (Springer-Verlag, Berlin, 1983), p. 277.
[19]R. Frahm, R. Haensel, and P. Rabe, in Ref. 18, p. 107.
[20]J. Kortright, W. Warburton, and A. Bienenstock, in Ref. 18, p. 362.